ORIGINAL PAPER

The design of new process, parametric analysis, technical and economic analysis of methanol production from biogas

Lei Zhu[1] · Ying Wang[2] · Yan Wang[1,3] · Zhixin Wang[4]

Abstract

In this study, a new process for producing methanol from biogas is presented. The process flowsheet was developed using Aspen HYSYS software, and sensitivity analysis of functional parameters was performed. In exergy analysis, the proposed process has an overall efficiency of 54.11%, in which the integration of the steam cycle plays an important role. The results also indicated that the overall exergy destruction rate is equal to 90527.02 kW, where the reformer and burner with 29% and 51% have the highest share in exergy destruction. Energy evaluation showed that the overall efficiency of converting biogas to methanol is 48.07%, and the intensity of losses per kilogram of methanol production is equal to 0.025 GJ. The economic analysis for the process was also carried out, and it was found that the production cost of each kilogram of methanol is equal to $ 286 with an annual profit of 1.2M\$ and its lowest selling price is 0.31 US\$/kg_{MeOH}. In addition, according to the simulation results, the value of methanol production from biogas is equal to 0.619kg_{MeOH}/kg_{biogas}.

Keywords Biogas · Economic analysis · Energy efficiency · Exergy analysis · Methanol production

1 Introduction

Methanol is one of the promising chemical materials which has various advantages. It can be directly used in the production of several chemicals, such as propylene, dimethyl ether, ethylene, dimethyl ether, and olefins (Hamelinck et al. 2004; Swain et al. 2011). Methanol has been proven to be an ideal engine fuel in numerous vehicles. Methanol is one of the most important raw materials in the petrochemical and chemical industry, with a forecasted demand of 117 Mtons in the near future (Patel et al. 2021). Im-orb et al. (2020) used a model developed in Aspen Plus V8.8 to simulate Biomethanol production from oil palm residues via gasification process. Oil palm residues were tested as to raw materials for

syngas production. Hernández and Martín (2016) evaluated the possibility of using biogas to produce methanol through the combination of steam reforming and dry reforming. Patel et al. (2018) suggested that biogas with an appropriate CH_4 to CO_2 ratio could act as a proper raw material to produce methanol by methanotrophs. Chen et al. (2019) suggested an integrated process of coal gasification and coking to methanol production (CGCTM). Dai et al. (2017) performed an exergy analysis to evaluate the performance of chemical production from entrained-bed gasification and Victorian brown coal through a process combining pyrolysis. The results showed that the exergy efficiency in this process was 4.5% higher than that of a conventional drying-gasification process and 1.5% higher than drying gasification that used a feed containing 25 wt% of lignite. Firmansyah et al. (2018) proposed wind energy by combining biomass for power system and production of methanol. Three methods of biomass utilization were considered, including oxy-fuel combustion, integrated gasification combined cycle with carbon capture, and biomass gasification process. Herdem et al. (2020) simulated the methanol production via carbon dioxide hydrogenation and proposed a novel system based on a combined non-combustion heat-carrier oxy-fuel combustion. dos Santos et al. (2018) proposed a new process for methanol production using biogas as a feedstock, consisting

✉ Yan Wang
  wangyan@eurasia.edu

[1] School of Business Administration, Xi'an Eurasia University, Xi'an 710065, Shaanxi, China

[2] EAAD School of Art and Design, Xi'an Eurasia University, Xi'an 710065, Shaanxi, China

[3] School of Economics and Finance, Xi'an Jiaotong University, Xi'an 710061, Shaanxi, China

[4] School of Economics, Hebei University, Baoding 071002, Hebei, China

of two steps: methanol synthesizing from syngas and biogas reforming. They examined different operating conditions (pressure and reactor temperature) to maximize methanol production. Anicic et al. (2014) compared two methods for methanol syntheses (direct methanol synthesis and two-step methanol synthesis) using carbon dioxide as the starting material. Direct synthesis was shown to have higher energetic and economic efficiency, but the difference can be ignored in terms of energy efficiency.

Methanol can be produced by the hydrogenation of carbon dioxide and carbon monoxide using catalysts, which is also mature technology (Herdem et al. 2019). Blumberg et al. (2019) investigated the environmental impact of commercial methanol production synthesis methods by producing syngas with auto thermal reforming and steam reforming. Many researchers have developed methanol synthesis catalysts for the use of residual gases in the steel and iron industry. For instance, Umchoo et al. (2018) performed an external magnetic field for the improvement of the catalytic activity selectivity of 10Fe10Cu/core–shell and 10Fe10Cu/infiltrate in terms of developing methanol synthesis catalysts with intrinsic magnetic properties in CO_2 hydrogenation to DME and methanol. Schittkowski et al. (2018) examined the challenges of using industrial $Al_2O_3Cu/ZnO/$catalysts to produce methanol using the byproduct gases in steel works. A partial thermochemical process, gasification, is considered the most cost-effective and efficient process for converting lignocellulosic biomass to synthesis gas (syngas), which can be used directly as the medium for synthesizing various biofuels and biochemical or as a fuel. Im-orb and Arpornwichanop (2020) used CO_2 recycled from the CO_2 capture unit into the gasifier and examined how different amounts would affect a process that combined gasification, biomass pyrolysis, and methanol synthesis. Although the energy consumption showed the opposite trend but the results showed that the yield of methanol increases with increasing recycled CO_2. Kalinci et al. (2010) found that the nature of biomass affected the gas composition, as well as exergy efficiencies and the energy of the process. Due to the using of high nitrogen contained-biomass, the exergy and energy efficiencies of the system decreases based on the low heating value of nitrogen. Several studies have been performed to overcome the economic and technical limitations of methanol synthesis from biomass/residues. Carvalho et al. (2018) evaluated the techno-economic performance of methanol production by black liquor co-gasification and found that grade AA methanol could even be cost-competitive with untaxed gasoline when mixed with black liquor in a ratio of 50/50. Zhang et al. (2020) proposed an economic and optimization of three methanol production systems based on entrained flow gasification combined with solid oxide cells (SOCs). Lin et al. (2010) performed an economic analysis of the coal-based system for power and methanol production. They performed

the system including an IGCC, waste heat boiler, the low-pressure methanol synthesis technology (single-stage).

There are also many studies focused on the economic and environmental analysis of renewable methanol production from CO_2 systems. Szima and Cormos (2018) analyzed the techno-economic and environmental performance of methanol synthesis from captured CO_2 from its flue gas and free H_2 but entirely focused on methanol synthesis, economic aspects, and purification unit without considering the life cycle environmental impact. According to the literature review, the studies on the life cycle assessment of renewable methanol production from CO_2 are still limited (Herdem et al. 2020).

1.1 Main novelties and contributions

To the best of our knowledge, there is little research on thermo-economic analysis of methanol production process through a renewable energy source of biogas. Most studies concentrated on simulation of approach for methanol production via carbon dioxide hydrogenation and proposed results for a novel system based on combined non-combustion heat-carrier oxy-fuel combustion. Moreover, thermo-economic analysis of methanol production is still rare. Due to lots of research focused on the economic and environmental studies of renewable methanol production from CO_2 systems, we developed the process flow sheet using Aspen HYSYS software, and sensitivity analysis of operational parameters was performed.

2 Process description

The process of different parts of methanol production from biogas or biomethanol is shown in Fig. 1. The production process consists of the following parts:

- Biogas reforming: In this part, synthesis gas is delivered to the system from the factory, which is the main feed for methanol production.
- Steam cycle: It is used for waste heat recovery and converts the waste heat of reformer gases to electricity.
- Compression: In this part, the pressure of the synthesized gas increases in several stages of the compressor and reaches the desired value to perform methanol reactions.
- Methanol synthesis: The methanol reactor, which is filled with the commercial copper catalyst, is placed in this part of the process to perform hydrogenation reactions.
- Methanol separation: Methanol separation from light gases and water is done using a distillation tower in this part.
- Heating supply: In this part, reformer energy and reboiler energy of methanol distillation are provided by mixing
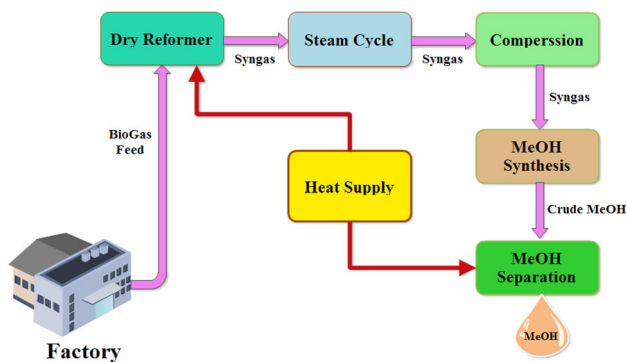
Fig. 1 Different parts of the biomethanol production process

combustion fuel (natural gas and produced gases from methanol separation) with the oxidizing agent (air).

Also, in Fig. 2, more detail of the process of biomethanol production from biogas is shown. Biogas, which is in ambient operating conditions, is first preheated by the HX1 heat exchanger and enters the reformer at atmospheric pressure. Where the reaction of methane and carbon dioxide produces synthesis gas. The biogas composition based on molar percentage is described as: CH_4: 38%, CO_2: 40%, and H_2: 22% (Hamelinck et al. 2004).

After performing the reforming reactions at the temperature of 950 °C and pressure of 1 atm (Benito et al. 2007), the synthetic gas enters the steam cycle at a lower temperature by passing through a heat exchanger (operating conditions in Table S1), where the energy of the hot gases of the reformer is used to generate electricity. The steam cycle has an evaporative heat exchanger (HX2), a steam turbine, a condensing heat exchanger (HX3), and a pump to circulate the working fluid (water). The synthesis gas leaves the steam cycle at a temperature of 45 °C and enters the compressors with intercoolers (using cooling water) to reach the desired pressure of 5000 kPa (Do and Kim 2019). Cooling water is used for cooling, because the outlet fluid from each stage of the compressor has a high temperature, so it must be cooled before entering the next stage of compression. For compression gas synthesis, K100 to K104 compressors are employed, and HX4 to HX7 heat exchangers are used for intercooling.

Since the operating conditions for the methanol reactor are a temperature of 250 °C and the pressure of 5000 kPa (Do and Kim 2019), the outlet flow of the K104 compressor is not cooled and entered the heat exchanger (HX8) at 172.9 °C. In HX8, using the outlet flow of the reactor, which is at a temperature of 250 °C, the temperature of the flow entering the reactor is increased to 240 °C. After that, the outlet flow of the methanol synthesis reactor enters the heat exchanger (HX9), where its temperature is reduced to 45 °C by the cooling water stream (CWS). The temperature reduction is performed owing to the condensation of methanol and

water from the vapor phase and the initial separation of light gases (Purge flow) using the V101 vertical two-phase separator. The vapor separated from the separator enters the burner as fuel to contribute to the production process and reduce fuel consumption. On the other hand, the liquid flow divided from the bottom of the V101 separator, which is called crude methanol, is fed to the distillation tower by passing through the expansion valve at a pressure of 120 kPa to obtain the separation and final production of methanol. The distillation column is tray type and has a partial condenser with steam and liquid products. From the top of the distillation tower drum reflux, light gas enters the burner to be used for combustion and heat generation. The liquid product is 100% methanol flow. From the distillation tower reboiler, the waste water, which has a small amount of methanol, is produced. As shown in Fig. 2, fuel flows (consisting of methane as natural gas, light gases above the distillation column, and excess gas above the V102 separator are provided to supply the heat needed for the dry reformer and methanol tower reboiler, and the resulting energy are provided to the equipment.

3 Process simulation

3.1 Simulation method

Aspen Hysys software is capable of providing professional flowsheets that is one of the most powerful software for simulating petrochemical processes. In this study, Aspen Hysys version 10 was used to simulate the biomethanol production process. In Fig. S1, the method of modeling biomethanol process in the Aspen software environment is presented.

The types of equipment that should be placed in the flowsheet are heat exchangers, simple cooler, plug reactor, Gibbs reactor, pressure reducing valve, partial condenser distillation tower, two-phase separator, turbine, compressor. First, each of these equipment needs to connect the input for convergence, output, and energy currents (if necessary) and second to enter the suitable operating characteristic (Spec) for each in the software. In heat exchangers, the temperature and pressure of inlet and outlet flow are suitable characteristics. Therefore, by changing pressure, convergence can be achieved by applying pressure to the outlet. In this simulation, the methanol separation distillation tower is tray type and has a partial condenser with liquid and vapor product. In Fig. 3, complete schematic of a simulation of the methanol production process, which was performed in the Aspen Hysys software, is shown. To simulate, several assumptions are considered as follows:

- The simulation is in a steady-state condition.
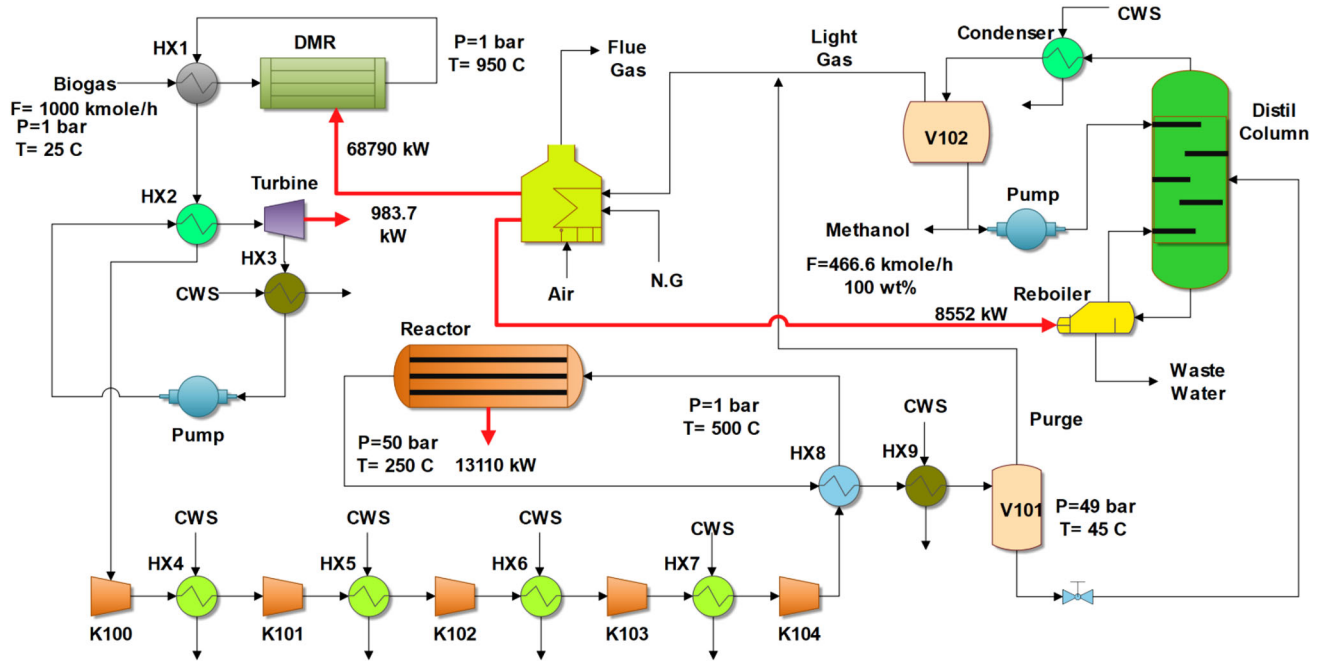- Adiabatic efficiency of pumps, compressors, and turbines equals 75%.

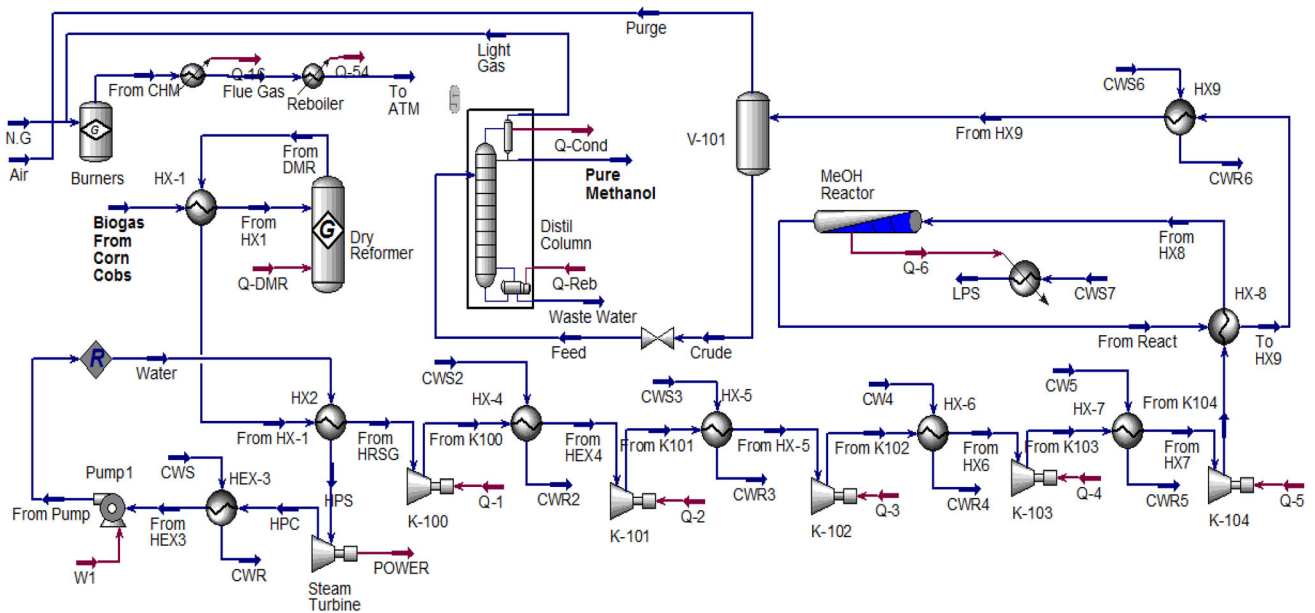**Fig. 2** Process flow diagram for biomethanol production

Fig. 3 Schematic diagram of the biomethanol production process

- The condensing temperature of the distillation column is 45 °C.
- The temperature of the outlet fluid of the compressors is a maximum of 150 °C.
- The cooling water temperature is 35 °C at the inlet and 40°C at the outlet.
- The inlet fuel to the burner only contains methane.
- The water pressure in the steam cycle is 12,000 kPa and the water in the HX2 is saturated steam.

- The outlet pressure of the operating fluid from the turbine equals 1000 kPa.
- The outlet temperature of the synthesis gas of the inter-coolers is equal to 45 °C.
- The temperature of the working fluid (water) at the inlet of the heat exchanger (HX2) is 38 °C.
- The pressure of the condenser and reboiler of the methanol separation tower is equal to 20 kPa.

Table 1 Conversion of biogas to synthetic gas using dry reforming (catalysts and operating conditions) (Yang and Ge 2016)

Input CH_4/CO_2	Catalyst	Temperature (°C)	Output H_2/CO	CH_4 conversion (%)	CO_2 Conversion (%)	Carbon formation mg/g-catalyst
0.5	Ce–Gd–O	800	1.07	50	88	–
0.8	Rh–Al	700	1.00	42	–	–
1	Mg–Al–Ni–La	700	0.76	80	82	–
1	Ni–Al	700	0.67	19	31	–
1	Ni–Pb–Al	700	0.88	60	78	–
1	Ni–Pb–1P–Al	700	0.77	55	71	–
1	Ni	700	1.0	54	66	41
1	Ni–La–Al	950	–	99	90	–

3.2 Fluid pack

This section is described in supplementary materials.

3.3 Modeling of synthesis reactors

3.3.1 Biogas reformer and burner energy production

In this simulation, the Gibbs reactor model is used to model the synthesis gas reactor and the burners that are responsible for supplying energy. Gibbs reactor calculates product density based on theoretical free energy minimum, which is a theoretical equilibrium composition (Ahoba-Sam et al. 2018). In the reformer, the following reaction occurs at the Ni–La–Al catalyst surface (Benito et al. 2007):

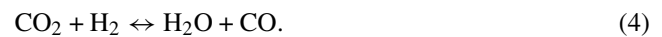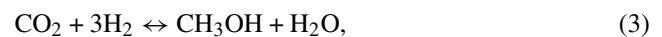$$CH_4 + CO_2 \rightarrow 2CO + 2H_2 \quad H^0 = 247 \text{ kj/mol}. \tag{1}$$

Dry reforming converts two stable molecules of methane and carbon dioxide into synthesis gas at 700–950 °C with the help of catalysts. Thermodynamically this operation is desirable at low pressure, and most studies have been done at a pressure of 1 atm or less. Biogas is a good source for this, because it contains methane and carbon dioxide together, and both carbon atoms in the final product are combined with increasing efficiency and reducing waste energy (Asencios et al. 2013). The catalyst used in dry reforming must first react with high activity and good stability under operating conditions and second prevent the formation of coke. Many studies used new and old catalysts, such as nickel (Lanzini et al. 2013; Serrano-Lotina et al. 2012; Serrano-Lotina and Daza 2014). Table 1 presents the types of catalysts and operating conditions are provided on each one that can be used in dry reforming.

3.3.2 Methanol synthesis reactor

In this study, we used catalytic–heterogeneous kinetics (commercial catalyst Cu/Zn/Al$_2$O$_3$) for the synthesis of methanol through hydrogenation of CO_2 and CO with high efficiency of methanol at low temperature (250 °C) and pressure of 5000 kPa. In addition, the Plug model reactor simulation is used to simulate the methanol synthesis reactor, and the Langmuir–Hinshelwood–Hougen–Watson kinetic method is used to define the reactions. On the other hand, the kinetic parameters used in the Langmuir–Hinshelwood–Hougen–Watson model were obtained through previous laboratory results (Abdelaziz et al. 2017). Methanol synthesis reactions are shown in Eqs. 2–4 (Abdelaziz et al. 2017; Do and Kim 2019; Zhang et al. 2018):

$$CO + 2H_2 \leftrightarrow CH_3OH, \tag{2}$$

$$CO_2 + 3H_2 \leftrightarrow CH_3OH + H_2O, \tag{3}$$

$$CO_2 + H_2 \leftrightarrow H_2O + CO. \tag{4}$$

Because the plug reactor has to be sized, the values provided by Abdelaziz et al. (2017) were used to size the methanol synthesis reactor. The reactor diameter is 5.5 m, the number of pipes is 3026, and the length of the pipes is 10 m in the simulation.

4 Process analysis

4.1 Energy efficiency

Energy efficiency for the biomethanol production process is defined as the sum of energy produced divided by the sum of input (consumption) energies (Eq. 5):

$$\eta_{\text{energy system}} = 100 \times \frac{\dot{m}_{\text{MeOH}} \text{LHV}_{\text{MeOH}} + \text{Energy Output}}{\dot{m}_{\text{biogas}} \text{LHV}_{\text{biogas}} + \text{Energy Input}}. \tag{5}$$

4.2 Exergy analysis

Exergy measures usefulness, energy quality, or potential for doing work (Hamrang et al. 2020). Exergy analysis is a suitable method for analyzing the amount of energy consumption, which is based on the second law of thermodynamics. Through this analysis, the inefficient parts of the system are identified (Ziapour et al. 2017). Exergy consists of four components: physical exergy $\left(E^{PH}\right)$, kinetic exergy $\left(E^{KN}\right)$, potential exergy $\left(E^{PT}\right)$ and chemical exergy $\left(E^{CH}\right)$. Kinetic and potential exergies are not usually considered in the calculations (Ahmadi et al. 2019). Physical exergy is the most achievable when the system from the initial state with temperature and pressure of T and P reaches physical equilibrium with the environment with temperature of T_0 and pressure P_0. The physical exergy of a closed system in a particular state is obtained by the following equation (Rostamzadeh et al. 2019):

$$e_{ph} = (h - h_0) - T_0(s - s_0), \tag{6}$$

where h and s are the enthalpy and specific entropy, respectively, and index 0 indicate the ambient condition of 25 °C and 101.3 kPa.

Chemical exergy is the most achievable when the system with the chemical temperature of T_0 and pressure of P_0, in addition to thermal and mechanical equilibrium, also reaches chemical equilibrium with the environment. Therefore, in addition to temperature and pressure, the chemical composition of the system must also be determined. Chemical exergy is defined by Eq. 7 (Mehrpooya and Zonouz 2017):

$$e_{ch} = \sum x_i e_i^0 + G - \sum x_i G_i. \tag{7}$$

In Eq. 7, x_i is the molar component of compound i in the material flow, e_i^0 is the standard chemical exergy of compound i in the flow, and G is the Gibbs free energy (dos Santos et al. 2018).

In this study, general exergy included only physical and chemical exergy, and the effect of two items, kinetic and potential exergy, was neglected. Table S2 presents the physical, chemical, and general exergies for the biomethanol production process. Also in Table S3 are the relationships related to exergy destruction and fuel exergy $(E_{x,F}^i)$ and product $(E_{x,P}^i)$ for the equipment used in the process flowsheet. Exergy destruction and exergy efficiency are the most important parameters for exergy analysis that are obtained through exergy balance for each equipment (Mehrpooya and Zonouz 2017). Exergy destruction $(\dot{E}_{x,D}^i)$ is calculated by the difference between the fuel exergy and the product exergy by Eq. 8 for each component. On the other hand, for component i, the

exergy efficiency is obtained by dividing the exergy of the product into fuel (Eq. 9):

$$\dot{E}_{x,D}^i = \dot{E}_{x,F}^i - \dot{E}_{x,P}^i, \tag{8}$$

$$\eta_{ex}^i = \frac{\dot{E}_{x,P}^i}{\dot{E}_{x,F}^i}. \tag{9}$$

In this study, to calculate the total exergy efficiency (η_{ex}^{total}) of the biomethanol production process, Eq. 10 is used. Where $\dot{E}_{MeOH}$ is the exergy of the methanol product, $\dot{W}_{turbine}$ is the work produced by the steam cycle turbine, $\dot{E}_{Biogas}$ is the biogas exergy, and $\dot{E}_{N.G}$ is the exergy of the natural gas entering the burner:

$$\eta_{ex}^{total} = 100 \times \frac{\dot{E}_{x,P}^{total}}{\dot{E}_{x,F}^{total}} = \frac{\dot{E}_{MeOH} + \dot{W}_{turbine}}{\dot{E}_{Biogas} + \dot{E}_{N.G}}. \tag{10}$$

4.3 Economic analysis

To evaluate the indicators of the biomethanol production process, it is necessary to understand the investment cost of the main equipment, which is calculated according to Table 2 (Chen et al. 2019; Yang et al. 2012). Details of the calculations of each component are provided in Eq. 11 (Chen et al. 2019). In this study, Eq. 12 is used to calculate the total investment cost (TCI). The relative factor (RF_i) of the investment cost of ith component according to Table 3 (Chauvy et al. 2020) should be placed in TCI. The equipment investment cost (E_I) for dry reforming and methanol synthesis units (synthesis gas compression, methanol reactor, distillation column, and related equipment) are calculated by Eq. 11 (Chen et al. 2019):

$$E_I = \sum_j \beta \cdot E_{IJ}^r \cdot \left(\frac{S_j}{S_j^r}\right)^{sf}, \tag{11}$$

$$TCI = E_I \cdot \left(1 + \sum_{i=1}^n RF_i\right), \tag{12}$$

where E_I, TCI, and β are equipment investment cost, total investment cost, inside construction invoice, respectively. In addition, E_{Ij}^r, S_j^r, S_j, sf, RF_i are the investment of reference equipment from j unit, basis (reference) scale for unit j, usability scale of unit j, scale invoice, and relative factor, correspondingly.

To calculate the total cost of production, assumptions are considered, which can be seen in Table S4. Utilization and raw materials consumption are obtained based on simulation results with Aspen Hysys software. Therefore, the total cost of biomethanol production can be obtained through Eq. 13. On the other hand, it is assumed that biogas is obtained from

Table 2 Summary of investment information for main equipment (Chen et al. 2019; Yang et al. 2012)

Units	Criterion	S_j^r	sf	β	E_I(US $)
DMR	Material caloric value	716 MW	0.67	0.65	55, 700, 000
MeOH synthesis	Syngas input	10, 810 mol/s	0.67	1	18, 300, 000
Steam cycle	Electricity generation	59.2 MW	0.67	0.65	94, 700, 000

Table 3 Relative factors for investment cost (Chen et al. 2019)

Type	Item (i)	RF_i
Direct cost	Purchased equipment (delivered)	0.21
	Purchased equipment installation	0.10
	Piping	0.12
	Buildings (including services)	0.15
	Electrical systems	0.06
	Land	0.01
	Instrumentation and Controls	0.05
Indirect cost	Engineering and supervision	0.1
	Working Capital	0.17
	Construction expenses	0.09
	Contingency	0.07
	Contractor's fee	0.04
Fixed-capital investment		1
Working capital		0.17

Table 4 Results for calculating the total cost of biomethanol production and production cost intensity

Component	Cost (MM$/year)
Raw material cost	Fuel Gas = 9.81
Utility cost	Water = 12.27, electricity = 6.84
Operating labor	0.01739MM
Direct supervisory and clerical labor	0.0035
Maintenance and repairs	1.32
Operating supplies	0.2
Laboratory charges	0.00261
General expenses	5.221
Byproduct	0.88
Total product cost	34.8
Total product cost intensity (US$/kg_{MeOH})	0.286

the factory as waste material and is used as feed, as a result of which only the input raw material can be considered as a gaseous fuel entering the burner:

$$\text{Total Product Cost} = \text{Utility}_C + \text{Raw material}_C + \text{O\&M}_C + \text{D}_C + \text{GE}_C - \text{BP}_C. \quad (13)$$

In Eq. 13, $\text{O\&M}_C$ is the operation and maintenance costs, D_C is the depreciation cost, GE_C is the General factory costs, and BP_C is the cost of byproduct.

An investment cost (TCI) of 22M is estimated to be required for the biomethanol production process. On the other hand, in Table 4 of various items, the total cost of biomethanol production in MM$/year based on the mentioned relations is reported. According to the annual production of methanol through biogas, which has been determined using simulation equivalent to 12, 1842.5 tons, the total cost of production (TPCI) of methanol from biogas is equal to 0.286US$/kg_{MeOH}.

4.3.1 Calculating the minimum selling price

The minimum selling price (MSP) parameter has been used as a base term for competitive economic evaluation in the biomethanol production process. MSP Indicates the minimum selling price per kilogram of methanol produced. The MSP is the selling price of methanol at the point, where the total revenue and cost are equal. Total income includes tax, return on investment (ROI) and operating expenses. The ROI parameter depends on the total investment cost, interest rate, economic life of the project and is defined by the following equation (Do and Kim 2019):

$$\begin{aligned}
\text{ROI} &= \text{TCI} \times \frac{i \times (1+i)^r}{(1+i)^r - 1} \\
&= E_I \cdot \left(1 + \sum_{i=1}^{n} RF_i\right) \times \frac{i \times (1+i)^r}{(1+i)^r - 1},
\end{aligned} \quad (14)$$

where i is the interest rate, r is the project's economic life, and TCI is the total cost of the investment. The total revenue of the biomethanol production process can be calculated through Eq. 15. Income depends on tax, tax rate, return on investment (ROI), and TPC (Do and Kim 2019). After calculating the total revenue of the biomethanol production plan, tax should be determined as one of the parameters that play a role in the MSP relationship, for which Eq. 16 is defined. The tax

Table 5 Economic results for calculating MSP

Component	MM$/year
Revenue	36
Profit	1.2
Tax	0.42
Minimum Selling Price (MSP)	0.31 US$/kg$_{MeOH}$

is derived from the difference between the project profit and the factory depreciation multiplied by the tax rate (Do and Kim 2019):

$$\text{Revenue} = \frac{(\text{ROI} \times \text{Tax Rate}) + \text{TPC} (1 - \text{Tax Rate})}{1 - \text{Tax Rate}}, \quad (15)$$

$$\text{Tax} = (\text{Profit} - \text{Depreciation}) \times \text{Tax Rate}. \quad (16)$$

The main economic inputs are the interest rate (8%), the lifetime of the system (20 years), and the tax rate (35%) (Do and Kim 2019).

After calculating the overall revenue parameters of the system, tax and ROI can be measured based on Eq. 17 MSP competitive parameter. In Eq. 17, the parameter $\dot{m}_{MeOH\ Prod}$ is the mass flow rate of methanol produced from the separation distillation tower in kg/h. In addition, using Eq. 18, the total profit of the project is calculated in dollars per year (Do and Kim 2019). The results of the estimates for calculating the MSP parameter and other parameters are presented in Table 5. In addition, in Table 6, the comparative parameters of MSP for this study and previous works that have used different methods to convert carbon dioxide to methanol and provide hydrogen to react with carbon dioxide are compared.

$$\text{Minimum Selling Price}\left(\frac{\text{US\$}}{\text{kg}_{MeOH}}\right) = \frac{\text{ROI} + \text{TPC} + \text{Tax}}{\dot{m}_{MeOH\ Prod}}, \quad (17)$$

$$\text{Profit} = \text{Revenue} - \text{TPC}. \quad (18)$$

Fig. 4 Effect of reformer pressure on the percentage of carbon dioxide conversion

5 Sensitivity analysis of operational parameters

5.1 Investigating the effect of reformer pressure

In this part of the study, the effect of reformer pressure is analyzed. As shown in Fig. 4, with increasing pressure, the conversion rate of carbon dioxide in the reforming reaction decreases and this equilibrium reaction progresses towards raw materials. As a result, it is best to perform this reaction at low pressures.

According to Fig. 5, when dry reforming is performed at pressures higher than atmospheric, the energy consumption for syngas production is also reduced. This is due to a decrease in the conversion of carbon dioxide due to increased pressure. On the other hand, the dry reforming reaction is extremely endothermic, so by reducing the conversion percentage, less heat will be demanded by the reformer.

According to Fig. 6, at lower pressures, methanol production is higher. The reason for this is that, in the reformer, by reducing the pressure, the conversion rate of carbon dioxide will be higher, and as a result, the synthesis gas will be produced at a higher rate, and when more synthesis gas
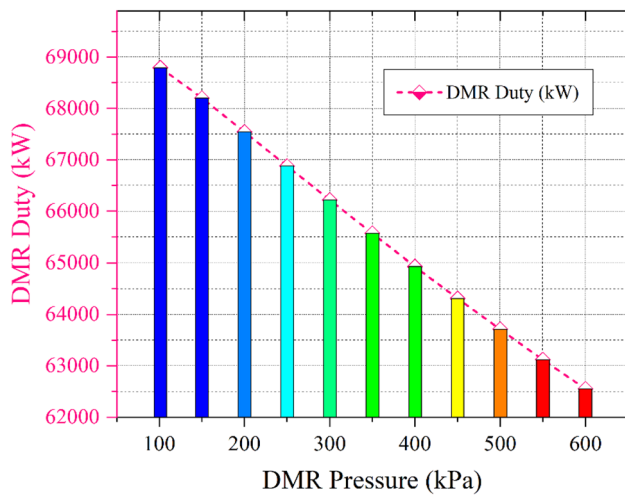
Table 6 Comparison of MSP competitive parameter

References	H$_2$ supply via	MeOH synthesis via	MSP (US$/kg$_{MeOH}$)
Do and Kim (2019)	Thermochemical H$_2$O splitting	Direct CO$_2$ hydrogenation	0.941
Kim et al. (2011)	Thermochemical H$_2$O splitting	Thermochemical CO$_2$ splitting	1.265
Alsayegh et al. (2019)	Photoelectrochemical H$_2$O splitting	Direct CO$_2$ hydrogenation	1.106
Current study	Biogas dry reforming	Direct CO$_2$ hydrogenation	0.31

Fig. 5 Effect of pressure on reformer energy consumption

Fig. 7 Effect of reformer temperature on the conversion rate of carbon dioxide

Fig. 6 Effect of reformer pressure on methanol production
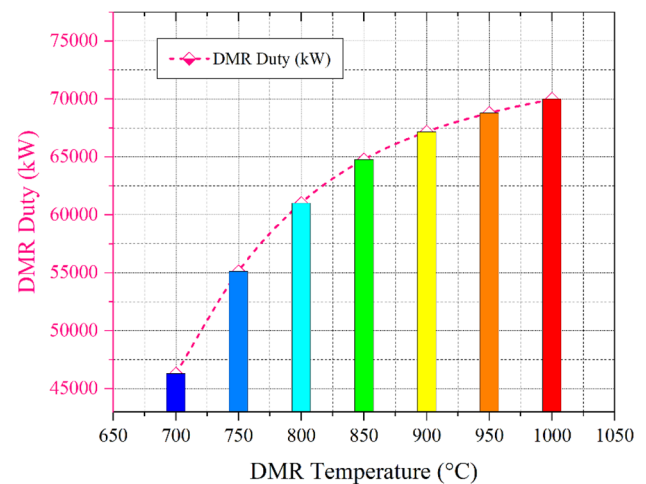
Fig. 8 Effect of reformer temperature on reformer energy consumption

is injected into the methanol reactor, methanol is removed from the reactor under reactions (Eqs. 3 and 4) and finally separated and produced through a distillation tower. Therefore, reducing the reformer pressure has a great effect on increasing methanol production.

5.2 Investigation of the effect of reformer temperature

The effect of reformer temperature (range 700–1000 °C) is analyzed in this part of the study. According to Fig. 7, increasing the temperature of the reformer has a significant effect on the conversion rate of carbon dioxide. This study was performed in a situation, where the reformer pressure is constant at each point and is equal to 101.3 kPa. In other words, when the reformer temperature rises at low pressure, it has an equilibrium reaction towards the production of synthesis gas. On
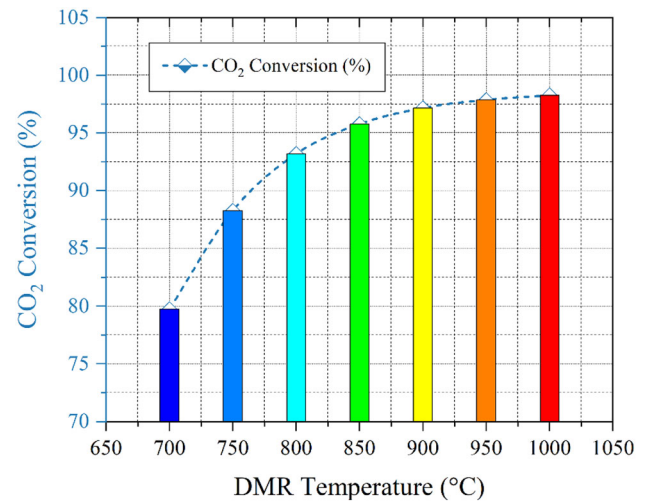
the other hand, according to Fig. 7, reducing the temperature of the reformer will greatly reduce the conversion rate of carbon dioxide, and this effect is much more tangible than the pressure. When comparing the conversion rate of carbon dioxide in the curve of Fig. 4 with Fig. 7, it is concluded that the effect of temperature relative to pressure on the rate of conversion of the dry reforming reaction is much more pronounced.

Figure 8 shows that when the temperature of the reformer increases, the energy consumption of this equipment also decreases. This indicates that it is better to increase the feed temperature to optimize the reformer, which requires the use of very large heat exchangers.

In addition, as shown in Fig. 9, the lower temperature of the reformer significantly reduces methanol production and vice versa. Studies show that the use of high temperature in the reformer is very suitable to increase the conversion
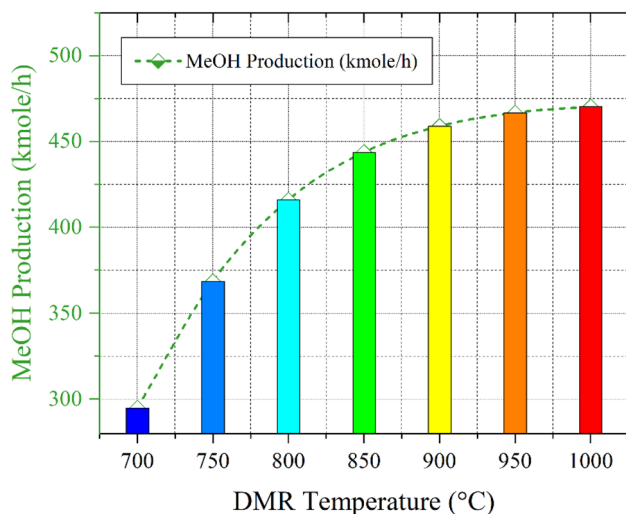
Fig. 9 Effect of reformer temperature on the intensity of methanol production

Table 7 Input and output energy of biomethanol production process

Inputs (kW)	
Furnace reformer fuel flow	66, 847.22
Pump	41.83
Compressors	
Cooling (cold utility)	27, 338
Input (food)	99, 510.44
Reboiler	Through the flue gas
Total	201, 321.49
Outputs (kW)	
Methanol Product	82, 681.81
Steam turbine power	983.7
Heat generated by methanol reactor	13, 110
Total	96, 775.51

rate of the dry reforming reaction, which causes more hydrogen to be sent to the methanol reactor and ultimately more methanol production. Therefore, to achieve higher production of methanol, the operating conditions governing the reformer must be such that, first, the temperature is high and second, the pressure is low. However, due to the existence of the steam cycle, which has been used to recover waste heat and generate electricity, increasing the inlet temperature of the reformer will reduce the temperature of the hot fluid in the HX2. In this way, less steam is generated to feed the turbine, which ultimately reduces the byproduct of the process (electricity). As a result, a trade-off limit should be set to raise the temperature of the reformer feed, so that, first, the temperature of the reformer does not decrease so much that coke formation and carbon dioxide conversion and finally methanol production decrease and second that it increases does not reduce the efficiency of the steam cycle and produce less electricity According to Table 1, the optimum temperature (allowable limit) for the reformer is $950°C$, which is also very suitable for the $\frac{CH_4}{CO_2}$ ratio in the incoming biogas (Corn Cobs), and from this temperature, coke formation is very low.

6 Results

In this study, Aspen HYSYS software was used for simulation. In addition to the energy balance (Table S1), the mass balance for the devices and the whole system is another result obtained through the Aspen HYSYS simulation flowsheet, which is tabulated in Table S5.

6.1 Energy evaluation results

Table 7 summarizes the consumed energies (hot and cold utilities) and the produced energies. In addition, the amount of energy loss can be calculated and measured through the difference between the sum of energy inputs and outputs. Another important parameter is the energy loss intensity (ELI), which can be calculated based on Eq. 19 (Leonzio 2018). In Eq. 19, Q_{inlet} is the input energy, Q_{outlet} is the energy produced and $\dot{m}_{MeOH\ Prod}$ is the intensity of methanol production:

$$\text{ELI}\ [\text{GJ}_{e,\text{lost}}/\text{kg}_{\text{MeOH}}] = \frac{\sum Q_{\text{inlet}} - \sum Q_{\text{outlet}}}{\dot{m}_{\text{MeOH Prod}}}. \tag{19}$$

According to the results presented in Table 7, the energy efficiency of the methanol production process from biogas is equal to 48.07%. In addition, the energy dissipation and energy loss intensity are 0.0454545 kW and 0.025 $\text{GJ}_{e,\ \text{lost}}/\text{kg}_{\text{MeOH}}$, respectively.

On the other hand, in Table 8, the comparison of total energy efficiency for this work with previous studies that were used different technologies is made. According to Table 8, methanol production from biogas is competing with solar technology, carbon dioxide hydrogenation, and biomass gasification in terms of energy efficiency. Comparison of the results with previous works shows that the use of biogas as a source for methanol production has a good performance in terms of energy efficiency. Therefore, since the energy and production costs of the product are interdependent, it can be said that biogas technology to methanol in terms of economic cost can be better or at least equal to these processes.

Table 8 Comparison of the results of this study with previous works

Reference work	Technology	Overall energy efficiency (%)
Milani et al. (2015)	SMR with CO_2 utilization	59
Blumberg et al. (2017)	Natural gas with CO_2 utilization	35.9
Tock et al. (2010)	Biomass Gasification	31.2
Wiesberg et al. (2019)	CO_2 Hydrogenation	38.7
Do and Kim (2019)	Direct CO_2 Hydrogenation using solar–thermal energy	47.1
This study	Biogas to methanol	48.07

6.2 Exergy evaluation results

Table 9 presents the exergy of fuel, the exergy of product, exergy destruction, and exergy efficiency for each component and the whole system. The rate of exergy destruction among heat exchangers for those heat exchangers that have used cooling water is much higher than the processors that have exchanged energy through process–process. In other words, the results show that when process–process heat exchangers are used (such as HX1, HX8, and HX2), the exergy destruction shows much lower values, and consequently, the exergy efficiency is also higher.

According to the exergy evaluation, Burner and Reformer have the highest exergy destruction among all types of equipment. According to Table 9, the total exergy destruction of the process is 90, 527.02 kW, with the share of Burner and Reformer of 51% and 27%, respectively. In fact, the burner is a part of the reformer, but in burner simulation, it is considered as a separate unit, so that it can be said the highest share of exergy destruction is for the reformer (78%) (Fig. 10). The pump and turbine have the lowest percentage of exergy destruction, but this does not necessarily mean that the efficiency of the turbine or pump is 100%. According to Table 9, the efficiency of the pump with the lowest exergy destruction share is equal to 10.85%.

According to Fig. 11, among the process components, the burner has the highest share of exergy destruction, followed by the reformer with a 21%. The main challenge of this process seems to be to reduce the exergy destruction in the dry reformer, which also has a great impact on the overall efficiency of the exergy. According to the results, the total exergy efficiency of the methanol production process from biogas is

Table 9 Fuel exergy, product exergy, exergy destruction rate, and exergy efficiency

| Component	$E_{x,D}^i$ (kW)	$E_{x,P}^i$ (kW)	$E_{x,F}^i$ (kW)	η_{ex}^i
HX1	1655.59	2362.37	4017.96	58.8
HX2	318.28	3312.48	3630.76	91.233
HX3	1902.1	247.56	2149.66	11.52
HX4	226.24	58.75	284.99	20.61
HX5	222.88	58.75	281.63	20.86
HX6	224.9	58.75	283.65	20.71
HX7	217.47	53.44	270.91	19.73
HX8	8.04	367.47	375.51	97.86
HX9	1364.1	249.25	1613.35	15.45
Pump1	36.82	4.48	41.3	10.85
Dry reformer	24437.46	23282.54	47720	48.79
Steam turbine	216.47	983.7	1200.17	81.96
MeOH reactor	8705.72	119867.65	128573.37	93.23
K100	270.56	1219.44	1490	81.84
K101	268.65	1210.35	1479	81.84
K102	270.29	1213.71	1484	81.79
K103	270.28	1215.72	1486	81.81
K104	283.77	1361.23	1645	82.75
Distil column	3738.44	1255.65	4994.09	25.14
Burner	45, 888.96	63, 170.6	109, 059.56	57.92
Cycle	$\sum E_{x,D}^i$ (kW)	$\sum E_{x,p}^i$ (kW)	$\sum E_{x,F}^i$ (kW)	η_{ex}^{total}
	90, 527.02	221, 553.89	312, 080.91	54.11

Main Units
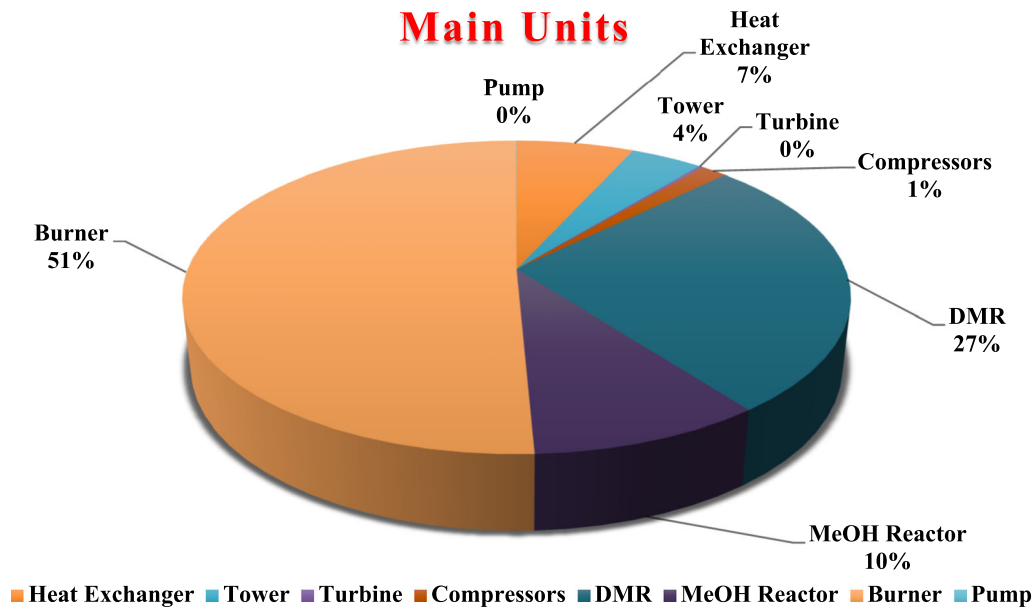
Fig. 10 Comparison of the percentage of exergy destruction of a single operation
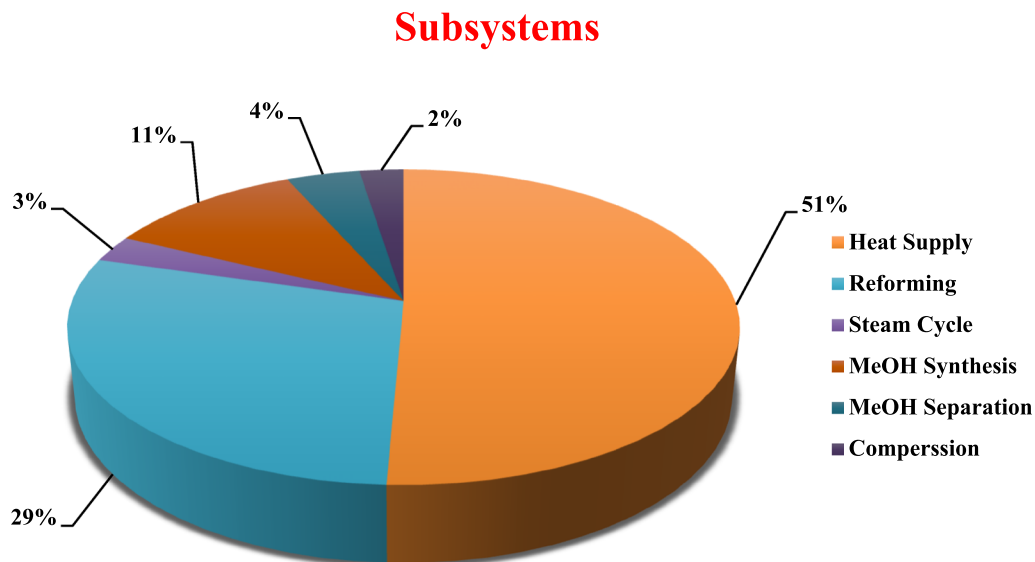
Subsystems

Fig. 11 Comparison of the percentage of destruction of different parts of the biomethanol production process

54.11%, in which the methanol reactor and HX8 and HX2 heat exchangers have a significant share. Methanol reactor has less exergy destruction compared to the reformer due to energy production, because, in the reformer, much energy must be given to the system to produce products.

7 Conclusion

In this study, the energy, exergy, and thermo-economic analyses of the methanol production process through a renewable energy source of biogas have been performed. Based on

the economic study, the cost of producing methanol from biogas is equal to 0.286 US $/kg_{MeOH}$. In terms of energy efficiency, the comparison indicated that the process of converting biogas to methanol could compete with technologies, such as solar, carbon dioxide hydrogenation, and biomass gasification, and in some cases, even better. According to the obtained results, the total energy efficiency was obtained to be 48.07% and the energy loss intensity was equal to $0.025 GJ_{e,lost}/kg_{MeOH}$. From the sensitivity analysis, it was found that the temperature of the reformer affects much more than its pressure on the conversion rate of carbon dioxide, reformer energy and methanol production rate. Parametric

analysis showed that dry biogas reforming at low pressure and high temperature is more efficient in terms of methanol production. Exergy analysis showed that the total exergy destruction is equal to 90, 527.02 kW, of which the share of reformer and burner is 21% and 57%, respectively. Studies also showed that the total exergy efficiency of this process is 54.11%. Comparison of the share of exergy destruction for components showed that in heat exchangers that use cooling water for cooling of the synthesis gas and other streams, the share of exergy destruction (67.72%) is much higher than other heat exchangers that hey work in a process–process (32.28%) streams.

References

Abdelaziz OY, Hosny WM, Gadalla MA, Ashour FH, Ashour IA, Hulteberg CP (2017) Novel process technologies for conversion of carbon dioxide from industrial flue gas streams into methanol. J CO2 Util 21:52–63

Ahmadi S, Ghaebi H, Shokri A (2019) A comprehensive thermodynamic analysis of a novel CHP system based on SOFC and APC cycles. Energy 186:115899. https://doi.org/10.1016/j.energy.2019.115899

Ahoba-Sam C, Øi LE, Jens KJ (2018) Process design of a novel low temperature methanol synthesis process using an air-blown autothermal reformer

Alsayegh S, Johnson JR, Ohs B, Wessling M (2019) Methanol production via direct carbon dioxide hydrogenation using hydrogen from photocatalytic water splitting: process development and techno-economic analysis. J Clean Prod 208:1446–1458

Anicic B, Trop P, Goricanec D (2014) Comparison between two methods of methanol production from carbon dioxide. Energy 77:279–289

Asencios YJO, Rodella CB, Assaf EM (2013) Oxidative reforming of model biogas over NiO–Y2O3–ZrO2 catalysts. Appl Catal B Environ 132:1–12

Benito M, García S, Ferreira-Aparicio P, Serrano LG, Daza L (2007) Development of biogas reforming Ni-La-Al catalysts for fuel cells. J Power Sources 169:177–183

Blumberg T, Morosuk T, Tsatsaronis G (2017) Exergy-based evaluation of methanol production from natural gas with CO2 utilization. Energy 141:2528–2539

Blumberg T, Lee YD, Morosuk T, Tsatsaronis G (2019) Exergoenvironmental analysis of methanol production by steam reforming and autothermal reforming of natural gas. Energy 181:1273–1284

Carvalho L, Lundgren J, Wetterlund E, Wolf J, Furusjö E (2018) Methanol production via black liquor co-gasification with expanded raw material base–Techno-economic assessment. Appl Energy 225:570–584

Chauvy R, Dubois L, Lybaert P, Thomas D, De Weireld G (2020) Production of synthetic natural gas from industrial carbon dioxide. Appl Energy 260:114249

Chen J, Yang S, Qian Y (2019) A novel path for carbon-rich resource utilization with lower emission and higher efficiency: an integrated process of coal gasification and coking to methanol production. Energy 177:304–318

Dai B, Zhang L, Cui J, Hoadley A, Zhang L (2017) Integration of pyrolysis and entrained-bed gasification for the production of chemicals from Victorian brown coal—process simulation and exergy analysis. Fuel Process Technol 155:21–31

Do TN, Kim J (2019) Process development and techno-economic evaluation of methanol production by direct CO2 hydrogenation using solar-thermal energy. J CO2 Util 33:461–472

dos Santos RO, de Sousa Santos L, Prata DM (2018) Simulation and optimization of a methanol synthesis process from different biogas sources. J Clean Prod 186:821–830

Firmansyah H, Tan Y, Yan J (2018) Power and methanol production from biomass combined with solar and wind energy: analysis and comparison. Energy Procedia 145:576–581

Hamelinck CN, Faaij APC, den Uil H, Boerrigter H (2004) Production of FT transportation fuels from biomass; technical options, process analysis and optimisation, and development potential. Energy 29:1743–1771

Hamrang F, Shokri A, Mahmoudi SMS, Ehghaghi B (2020) Performance analysis of a new electricity and freshwater production system based on an integrated gasification combined cycle and multi-effect desalination. Sustainability. https://doi.org/10.3390/su12197996

Herdem MS, Sinaki MY, Farhad S, Hamdullahpur F (2019) An overview of the methanol reforming process: comparison of fuels, catalysts, reformers, and systems. Int J Energy Res 43:5076–5105

Herdem MS, Mazzeo D, Matera N, Wen JZ, Nathwani J, Hong Z (2020) Simulation and modeling of a combined biomass gasification-solar photovoltaic hydrogen production system for methanol synthesis via carbon dioxide hydrogenation. Energy Convers Manag 219:113045

Hernández B, Martín M (2016) Optimal process operation for biogas reforming to methanol: effects of dry reforming and biogas composition. Ind Eng Chem Res 55:6677–6685

Im-orb K, Arpornwichanop A (2020) Process and sustainability analyses of the integrated biomass pyrolysis, gasification, and methanol synthesis process for methanol production. Energy 193:116788

Im-orb K, Phan AN, Arpornwichanop A (2020) Bio-methanol production from oil palm residues: a thermodynamic analysis. Energy Convers Manag 226:113493

Kalinci Y, Hepbasli A, Dincer I (2010) Efficiency assessment of an integrated gasifier/boiler system for hydrogen production with different biomass types. Int J Hydrogen Energy 35:4991–5000

Kim J, Henao CA, Johnson TA, Dedrick DE, Miller JE, Stechel EB, Maravelias CT (2011) Methanol production from CO2 using solar-thermal energy: process development and techno-economic analysis. Energy Environ Sci 4:3122–3132

Lanzini A, Leone P, Guerra C, Smeacetto F, Brandon NP, Santarelli M (2013) Durability of anode supported Solid Oxides Fuel Cells (SOFC) under direct dry-reforming of methane. Chem Eng J 220:254–263

Leonzio G (2018) State of art and perspectives about the production of methanol, dimethyl ether and syngas by carbon dioxide hydrogenation. J CO2 Util 27:326–354

Lin H, Jin H, Gao L, Han W (2010) Economic analysis of coal-based polygeneration system for methanol and power production. Energy 35:858–863

Mehrpooya M, Zonouz MJ (2017) Analysis of an integrated cryogenic air separation unit, oxy-combustion carbon dioxide power cycle and liquefied natural gas regasification process by exergoeconomic method. Energy Convers Manag 139:245–259

Milani D, Khalilpour R, Zahedi G, Abbas A (2015) A model-based analysis of CO2 utilization in methanol synthesis plant. J CO2 Util 10:12–22

Patel SKS, Kondaveeti S, Otari SV, Pagolu RT, Jeong SH, Kim SC, Cho B-K, Kang YC, Lee J-K (2018) Repeated batch methanol production from a simulated biogas mixture using immobilized *Methylocystis bryophila*. Energy 145:477–485

Patel SKS, Gupta RK, Kalia VC, Lee J-K (2021) Integrating anaerobic digestion of potato peels to methanol production by methanotrophs immobilized on banana leaves. Bioresour Technol 323:124550

Rostamzadeh H, Ebadollahi M, Ghaebi H, Shokri A (2019) Comparative study of two novel micro-CCHP systems based on organic Rankine cycle and Kalina cycle. Energy Convers Manag 183:210–229

Schittkowski J, Ruland H, Laudenschleger D, Girod K, Kähler K, Kaluza S, Muhler M, Schlögl R (2018) Methanol synthesis from steel mill exhaust gases: challenges for the industrial $Cu/ZnO/Al_2O_3$ catalyst. Chemie Ing Tech 90:1419–1429

Serrano-Lotina A, Daza L (2014) Influence of the operating parameters over dry reforming of methane to syngas. Int J Hydrogen Energy 39:4089–4094

Serrano-Lotina A, Martin AJ, Folgado MA, Daza L (2012) Dry reforming of methane to syngas over La-promoted hydrotalcite clay-derived catalysts. Int J Hydrogen Energy 37:12342–12350

Swain PK, Das LM, Naik SN (2011) Biomass to liquid: a prospective challenge to research and development in 21st century. Renew Sustain Energy Rev 15:4917–4933

Szima S, Cormos C-C (2018) Improving methanol synthesis from carbon-free H2 and captured CO_2: a techno-economic and environmental evaluation. J CO2 Util 24:555–563

Tock L, Gassner M, Maréchal F (2010) Thermochemical production of liquid fuels from biomass: thermo-economic modeling, process design and process integration analysis. Biomass Bioenerg 34:1838–1854

Umchoo W, Sriakkarin C, Donphai W, Warakulwit C, Poo-arporn Y, Jantaratana P, Witoon T, Chareonpanich M (2018) Green and sustainable methanol production from CO2 over magnetized FeCu/core–shell and infiltrate mesoporous silica-aluminosilicates. Energy Convers Manag 159:342–352

Wiesberg IL, Brigagão GV, Ofélia de Queiroz FA, de Medeiros JL (2019) Carbon dioxide management via exergy-based sustainability assessment: carbon capture and storage versus conversion to methanol. Renew Sustain Energy Rev 112:720–732

Yang L, Ge X (2016) Biogas and syngas upgrading. Advances in bioenergy. Elsevier, Oxford, pp 125–188

Yang S, Yang Q, Li H, Jin X, Li X, Qian Y (2012) An integrated framework for modeling, synthesis, analysis, and optimization of coal gasification-based energy and chemical processes. Ind Eng Chem Res 51:15763–15777

Zhang C, Jun K-W, Gao R, Kwak G, Park H-G (2018) Efficient way of carbon dioxide utilization in a gas-to-methanol process: from fundamental research to industrial demonstration. Top Catal 61:1794–1809

Zhang H, Wang L, Perez-Fortes M, Maréchal F, Desideri U (2020) Techno-economic optimization of biomass-to-methanol with solid-oxide electrolyzer. Appl Energy 258:114071

Ziapour BM, Saadat M, Palideh V, Afzal S (2017) Power generation enhancement in a salinity-gradient solar pond power plant using thermoelectric generator. Energy Convers Manag 136:283–293